

Simultaneous substitution of Ba, Mn and Co into Fe₃O₄ spinel structure: magnetic and electrochemical sensing properties of the synthesized nanoparticles

Nadir S E Osman*¹, Neeta Thapliyal², Thomas Moyo¹ and Rajshekhar Karpoormath²

¹School of Chemistry and Physics, Westville campus, University of KwaZulu-Natal, Durban 4000, South Africa

²Department of Pharmaceutical Chemistry, Discipline of Pharmaceutical Sciences, College of Health Sciences, University of KwaZulu-Natal, Durban 4000, South Africa

E-mail: osmann@ukzn.ac.za

Abstract. Single phase structured Ba_{1/3}Mn_{1/3}Co_{1/3}Fe₂O₄ nanoferrite was synthesized. The phase formation was confirmed by X-ray diffraction. The morphology and particle distribution of the synthesized nanoferrite particles were observed using transmission electron microscopy. The magnetic hyperfine parameters were obtained from room temperature ⁵⁷Fe Mössbauer spectroscopy. Vibrating sample magnetometer measurements were performed to investigate the magnetic properties of the sample. The electrochemical properties of the sample were also investigated. Cyclic voltammograms of ferricyanide oxidation showed that the modified electrode by Ba_{1/3}Mn_{1/3}Co_{1/3}Fe₂O₄ nanoparticles exhibited improved electrochemical activity as compared to the bare electrode. These high-performance electrodes are expected to lead to the development of a novel group of electrochemical sensors.

1. Introduction

Spinel ferrites have several properties [1] which make them useful in many applications such as in photoelectric devices [2], microwave devices [3, 4], catalysis [5] and sensors [6]. Electrical and magnetic properties of spinel ferrites depend on their chemical composition, cation distribution and synthesis method. In this respect numerous efforts have been undertaken in order to improve the basic properties of spinel ferrites [7]. It is known that by substituting different ions in spinel ferrite structure, their magnetic and electrical properties can be changed [8-9]. In the present work, we have synthesized a single phase structure of Ba_{1/3}Mn_{1/3}Co_{1/3}Fe₂O₄ ferrite nanoparticles and investigate the associated structural, magnetic and electrochemical properties.

2. Experimental details

The Ba_{1/3}Mn_{1/3}Co_{1/3}Fe₂O₄ ferrite nanoparticle sample was produced by glycol-thermal technique using a Watlow series model PARR 4843 stirred pressure reactor. The starting materials were high purity (BaCl₂·6H₂O: 99 %, MnCl₂·4H₂O: 99 %, CoCl₂·4H₂O: 98 % and FeCl₂·6H₂O: 99 %) all purchased from Sigma-Aldrich. A well-mixed solution of the starting materials was precipitated with NH₄OH solution until a PH of 9.0 was reached. Details of the synthesis method have been reported elsewhere [10]. The phase and structural characterizations of the sample was obtained by a Phillips X-ray diffractometer type Model: PANalytical, EMPYREAN using CoK α radiation. The morphology and micro-structure of

the nanoparticles were investigated by high-resolution transmission electron microscopy (HRTEM) (type: Jeol_JEM-1010). ^{57}Fe Mössbauer spectra were obtained by a conventional spectrometer using a ^{57}Co source sealed in Rh matrix and vibrated at constant acceleration. Magnetic measurements were performed at room temperature using a LakeShore model 735 vibrating sample magnetometer (VSM). Potassium ferricyanide and potassium chloride were supplied by Merck. The voltammetric experiments were conducted on an electrochemical analyzer (800B Series, CH Instruments, Inc.) in a three-electrode electrochemical cell, consisting of a Ag/AgCl reference electrode, a platinum counter electrode $\text{Ba}_{1/3}\text{Mn}_{1/3}\text{Co}_{1/3}\text{Fe}_2\text{O}_4/\text{GCE}$ and a bare/modified glassy carbon working electrode. The modified electrode was prepared by drop-casting a 0.5 mg/mL solution of $\text{Ba}_{1/3}\text{Mn}_{1/3}\text{Co}_{1/3}\text{Fe}_2\text{O}_4$ nanoparticles in dimethylformamide (DMF) solvent onto the electrode surface.

3. Results and discussion

Figure 1(A) shows XRD patterns of the synthesized nanoparticles. All the peaks are well indexed based on spinel structure (JCPDS file No. 22-1086) [11]. No impurity peaks were observed on the XRD pattern. The highest peak intensity in Figure 1 was identified as 311 and was used to calculate the lattice parameter a using Bragg's equation $a = d(h^2 + k^2 + l^2)^{1/2}$ where d is the inter-planar spacing and hkl are the Miller indices [12]. The average crystalline size D was calculated using Scherrer's formula $D = 0.9\lambda / \beta \cos \theta$, where β is the full-width at half-maximum of the (311) XRD peak and θ is the Bragg's angle [13]. The microstrain ζ was determined using the Williamson-Hall plot [14]. The calculated values of the lattice parameter, crystallite size and microstrain for the as-prepared $\text{Ba}_{1/3}\text{Mn}_{1/3}\text{Co}_{1/3}\text{Fe}_2\text{O}_4$ were found to be 0.839 ± 0.003 nm, 8.37 ± 0.06 nm and 0.0015 ± 0.00012 , respectively. The morphology of the synthesized nanoparticles was investigated by high resolution transmission microscopy (HRTEM). The synthesized nanoparticles show a degree of shape uniformity. Furthermore, some agglomeration is observed as it seen from Figure 1(B). The average particles size of 9 ± 2 nm was estimated from the HRTEM image.

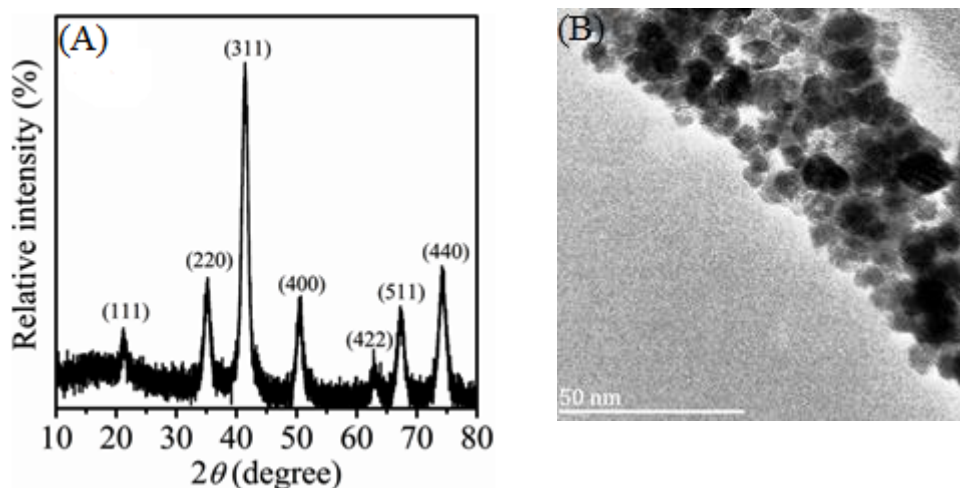


Figure 1. (A) X-ray diffraction patterns and (B) HRTEM images for as-prepared $\text{Ba}_{1/3}\text{Mn}_{1/3}\text{Co}_{1/3}\text{Fe}_2\text{O}_4$ ferrite nanoparticles.

Figure 2 shows the magnetic properties of the as-prepared $\text{Ba}_{1/3}\text{Mn}_{1/3}\text{Co}_{1/3}\text{Fe}_2\text{O}_4$ investigated at room temperature by Mössbauer spectroscopy and magnetization measurement. In Figure 2(A), the

Mössbauer spectrum is fitted by two Zeeman sextets which are related to the iron ions in tetrahedral A and octahedral B sites [15]. The s-shape magnetization is consistent with superparamagnetic behavior.

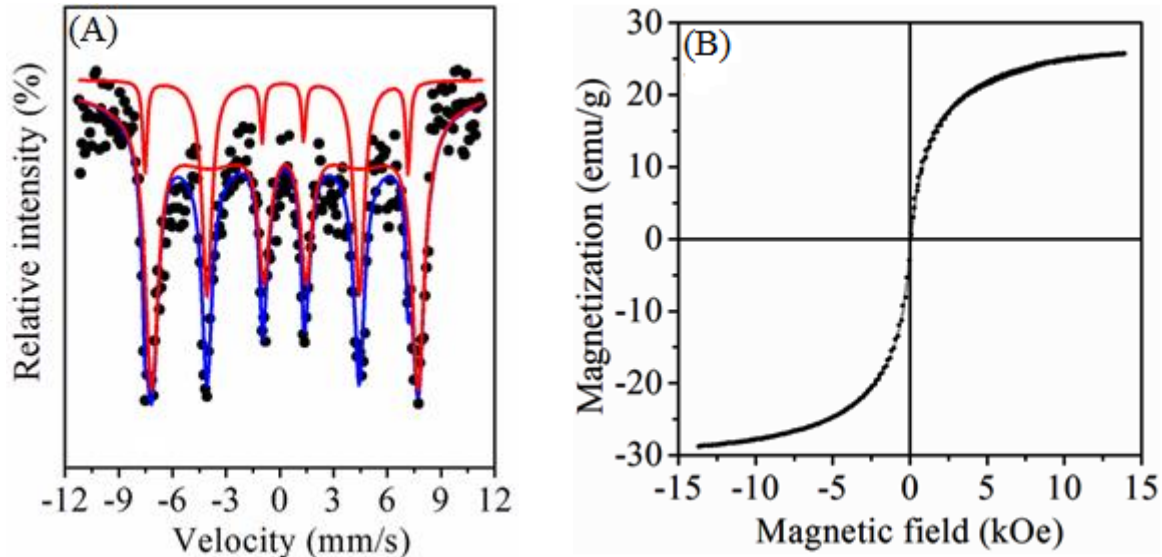


Figure 2. Room temperature Mössbauer measurement (A) and typical magnetic hysteresis loop measure at room temperature (B).

The magnetic hyperfine fields (H) were calculated to be 456 ± 3 kOe and 462 ± 3 kOe at A- and B-sites, respectively. The values of H are expected to be high due to super-exchange interactions between the atomic moments of the sample [16]. The isomer shift value at B-site is greater than at A-site. This is because of the bond separation between O^{2-} and Fe^{3+} is larger at B-site [17]. Hence the overlapping of Fe^{3+} ion orbitals is smaller at B-site. The magnetic hyperfine parameters are presented in Table 1.

Table 1. Isomer shifts (δ), hyperfine magnetic fields (H), line widths (Γ) and Fe^{2+} fraction population (f) on A-site and Fe^{3+} on B- site for $Ba_{1/3}Mn_{1/3}Co_{1/3}Fe_2O_4$ nanoparticles.

Site	δ (mm/s)	H (kOe)	Γ (mm/s)	f (%)
A	0.09 ± 0.0	456 ± 3	0.13 ± 0.04	18.4
B	0.39 ± 0.1	462 ± 3	0.38 ± 0.02	81.6

The magnetic hysteresis loop of the as-prepared $Ba_{1/3}Mn_{1/3}Co_{1/3}Fe_2O_4$ was carried out in an external applied magnetic field of about 14 kOe at 300 K. The M - H (where M is the magnetization) curve (Figure 2 (B)) has a coercivity value of 43 ± 1 Oe. The obtained values of maximum magnetization, remanence and hysteresis loop squareness are 27 ± 2 emu/g, 1.5 ± 0.1 emu/g and 0.037, respectively.

The electrochemical activity of the synthesized $Ba_{1/3}Mn_{1/3}Co_{1/3}Fe_2O_4$ nanoparticles was investigated using potassium ferricyanide $K_3[Fe(CN)_6]$ as the redox probe. Figure 3 A shows the cyclic voltammetric response observed at bare glassy carbon electrode (GCE) and $Ba_{1/3}Mn_{1/3}Co_{1/3}Fe_2O_4$ /GCE in the presence of 1 mM $K_3[Fe(CN)_6]$ in 0.1 M KCl solution. Well-defined redox peaks were observed at both electrodes. However, the $Ba_{1/3}Mn_{1/3}Co_{1/3}Fe_2O_4$ /GCE was found to exhibit improved electrochemical behavior, exhibiting an increased peak current response and a negative shift in peak potential, as

compared to the bare electrode. This suggests that the $\text{Ba}_{1/3}\text{Mn}_{1/3}\text{Co}_{1/3}\text{Fe}_2\text{O}_4$ nanoparticles effectively electrocatalyze the redox process of $\text{K}_3[\text{Fe}(\text{CN})_6]$. This is attributed to an enhanced rate of electron transfer owing to excellent electrical conductivity and high surface area of the synthesized $\text{Ba}_{1/3}\text{Mn}_{1/3}\text{Co}_{1/3}\text{Fe}_2\text{O}_4$ nanoparticles.

To establish that $\text{Ba}_{1/3}\text{Mn}_{1/3}\text{Co}_{1/3}\text{Fe}_2\text{O}_4$ nanoparticles improve the surface area of the electrode, the effective surface area (A) of bare GCE and $\text{Ba}_{1/3}\text{Mn}_{1/3}\text{Co}_{1/3}\text{Fe}_2\text{O}_4/\text{GCE}$ were determined by recording cyclic voltammograms in 1.0 mM $\text{K}_3[\text{Fe}(\text{CN})_6]$ solution at different sweep rates (Figure 3 B). Using the Randles-Sevcik equation: $i_p = 2.69 \times 10^5 n^{3/2} A D^{1/2} C v^{1/2}$ where i_p is the peak current (in Amperes), n is the number of electrons transferred in the electrochemical process, D (in $\text{cm}^2 \text{s}^{-1}$) is the diffusion coefficient ($D = 7.6 \times 10^{-6} \text{ cm}^2 \text{s}^{-1}$ for $[\text{Fe}(\text{CN})_6]^{3-}$), C (in mol cm^{-3}) is the concentration of the electroactive species and v is the scan rate (in V s^{-1}) and employing the slope of i_{pa} versus $v^{1/2}$ plot (inset of Figure 3 B), Surface area was found to be 0.070 cm^2 and 0.218 cm^2 for bare GCE and $\text{Ba}_{1/3}\text{Mn}_{1/3}\text{Co}_{1/3}\text{Fe}_2\text{O}_4/\text{GCE}$, respectively. The surface area of the modified electrode was at least 3 times larger than that of the bare GCE electrode, indicating superior conductivity of the $\text{Ba}_{1/3}\text{Mn}_{1/3}\text{Co}_{1/3}\text{Fe}_2\text{O}_4$ nanoparticles. Thus, it is expected that the novel nanoferrites can lead to the development of a new group of electrochemical sensors.

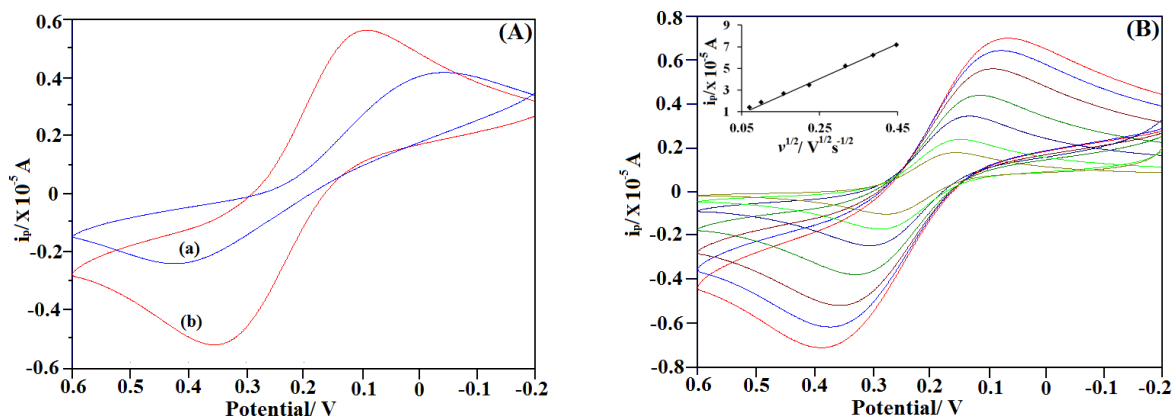


Figure 3 (A) Cyclic voltammograms of 1.0 mM $\text{K}_3[\text{Fe}(\text{CN})_6]$ in 0.1 M KCl solution at (a) bare GCE and (b) $\text{Ba}_{1/3}\text{Mn}_{1/3}\text{Co}_{1/3}\text{Fe}_2\text{O}_4/\text{GCE}$ at 100 mV/s. (B) Cyclic voltammograms of 1.0 mM $\text{K}_3[\text{Fe}(\text{CN})_6]$ in 0.1 M KCl solution at $\text{Ba}_{1/3}\text{Mn}_{1/3}\text{Co}_{1/3}\text{Fe}_2\text{O}_4/\text{GCE}$ at sweep rates 5–200 mV s^{-1} (Inset displays plot of peak current versus square root of sweep rate).

4. Conclusions

$\text{Ba}_{1/3}\text{Mn}_{1/3}\text{Co}_{1/3}\text{Fe}_2\text{O}_4$ nanoparticles ferrite was successfully produced by glycol thermal method. The obtained values of lattice parameter, crystallite size and microstrain are found to be $0.839 \pm 0.003 \text{ nm}$, $8.37 \pm 0.06 \text{ nm}$ and 0.0015 ± 0.0001 respectively. We attribute the microstrain as due to the synthesis method and conditions. HRTEM images show that the synthesized nanoparticles have average particle sizes of $9 \pm 2 \text{ nm}$. This is close to the crystallite size estimated from the XRD measurements. The Mössbauer spectrum was fitted only with two sextets associated with the Zeeman splitting with Fe^{2+} and Fe^{3+} on A- and B-sites respectively. The synthesized sample shows small value of coercive field of $43 \pm 1 \text{ Oe}$ as deduced from the room temperature hysteresis loop. $\text{Ba}_{1/3}\text{Mn}_{1/3}\text{Co}_{1/3}\text{Fe}_2\text{O}_4$ nanoferrite modified electrode showed good electrocatalytic activity. These high-performance electrodes are expected to lead to the development of a novel group of electrochemical sensors.

Acknowledgments

The authors would like to thank the National Research Foundation (NRF) of South Africa for equipment grants, Department of Pharmaceutical Chemistry (College of Health Sciences, University of KwaZulu-Natal, South Africa) for financial support (NT) and Sudan University of Science and Technology for the study leave (NSEO).

References

- [1] Xu Q, Wei Y, Liu Y, Ji X, Yang L and Gu M 2009 *Solid State Sci.* **11(2)** 472-478
- [2] Hu J, Li L, Yang W, Manna L, Wang L and Alivisatos A P 2007 *J. Magn. Magn. Mater.* **308** 198
- [3] Baykal A, Kasapoglun, Durmus Z, Kavas H, Toprak M S and Koseoglu Y 2009 *Turk J Chem.* **33** 33-45
- [4] Gunjakar J L, More A M, Gurav K Vand Lokhande C D 2008 *Appl Surf Sci* **254(18)** 5844-5848
- [5] Sloczynski J, Janas J, Machej T, Rynkowski J and Stoch J 2000 *Appl Catal B* **24(1)** 45-60
- [6] Pena M A and Fierro J L G 2001 *Chem Rev* **101(7)** 1981-2018
- [7] Smit J and Wijn H P J 1959, *Ferrites* (Eindhoven: Netherlands) p 278–282
- [8] Goldman A 1999, *Handbook of Modern Ferromagnetic Materials* (New York: Springer)
- [9] Willard M A, Kurihara L K, Carpenter E E, Calvin S and Harris V G 2004 *Int. Mater. Rev* **49** 125-170
- [10] Osman N S E, Moyo T and Abdallah H M I 2014 *Proceedings of SAIP* 128-133 Available online at <http://events.saip.org.za>
- [11] Osman N S E, Thapliyal N, Alwan W S, Karpoormath R and Moyo T. 2015 *J Mater Sci: Mater Electron* **26** 5097-5105
- [12] Lemine O M, Bououdina M, Sajieddine M, Al-Saie A.M, Shafi M, Khatab A, Al-hilali M and Henini M 2011 *Physica B* **406** 1989–1994
- [13] Thapliyal N, Osman N S E, Patel H, Karpoormath R, Goyal R N, Moyo T and Patel R 2015 *RSC Advances* DOI: 10.1039/C5RA05286F
- [14] Salunkhe A B, Khot V M, Phadatare M R, Thorat N D, Joshi R S, Yadav H M and Pawar S H 2014 *J. Magn. Magn. Mater* **352** 91-98
- [15] Parvatheeswara Rao B, Subba Rao P S V, Murthy G V S and Rao K H 2004 *J. Magn. Magn. Mater* **268** 315–320
- [16] Ghasemi A, Jr A P and Machado C F C 2012 *J. Magn. Magn. Mater* **324** 2193–2198
- [17] Lakshman A, Subba Rao P S V, Rao KH 2006 *Mater Lett* **60** 7–10